PHYSICAL REVIEW E **90**, 041003(R) (2014)

Magnetic helicity and the evolution of decaying magnetohydrodynamic turbulence

Arjun Berera* and Moritz Linkmann†

SUPA, School of Physics and Astronomy, University of Edinburgh, Peter Guthrie Tait Road EH9 3FD, United Kingdom

(Received 2 June 2014; published 22 October 2014)

Ensemble-averaged high resolution direct numerical simulations of reverse spectral transfer are presented, extending on the many single realization numerical studies done up to now. This identifies this type of spectral transfer as a statistical property of magnetohydrodynamic turbulence and thus permits reliable numerical exploration of its dynamics. The magnetic energy decay exponent from these ensemble runs has been determined to be $n_E = (0.47 \pm 0.03) + (13.9 \pm 0.8)/R_\lambda$ for initially helical magnetic fields. We show that even after removing the Lorentz force term in the momentum equation, thus decoupling it from the induction equation, reverse spectral transfer still persists. The induction equation is now linear with an externally imposed velocity field, thus amenable to numerous analysis techniques. A new door has opened for analyzing reverse spectral transfer, with various ideas discussed.

DOI: 10.1103/PhysRevE.90.041003 PACS number(s): 47.27.ek, 52.65.Kj, 52.35.Ra

On large length scales kinetic plasma effects can be neglected and magnetohydrodynamics (MHD) gives a good first order approximation to plasma evolution. The relevance of MHD turbulence ranges from industrial application, fusion research, solar physics (e.g., coronal heating) to astrophysics and cosmology, where it might leave detectable signatures in astrophysical processes [1] and even for the very early universe the possibility of a large-scale primordial magnetic field [2–5]. While there are many applications of MHD turbulence research in the above areas, some of the theoretical problems still remain open. Fundamental research in MHD turbulence consists of many active fields such as the amplification of a seed magnetic field by dynamo processes [6], different proposed models concerning the scaling of the energy spectra taking small-scale anisotropy into account [7], and MHD turbulence decay, to name only a few.

Selective decay [8,9], that is the decay of ideal quadratic invariants of MHD flows at different rates, dominates the nonlinear evolution of decaying turbulent MHD flows. It is related to the direction of spectral transfer of said ideal invariants. The magnetic helicity, which is one of the three ideal invariants of MHD flows (the other two being the total energy and the cross helicity), has been shown to influence the evolution of the magnetic field [10,11] possibly through its reverse spectral transfer (RST)[1] [13]. An understanding of the underlying mechanism of RST remains elusive, though much progress has been made.

In this Rapid Communication we expand the numerical study of RST and its effects on MHD turbulence decay to ensemble-averaged data, which permits more reliable numerical exploration of the MHD equations compared to the single realization studies done up to now. We also deconstruct the nonlinear MHD equations and identify some of the underpinnings of RST. Here we treat incompressible MHD turbulence only, and the magnetic Prandtl number is set to unity.

The incompressible decaying MHD equations are

$$\partial_t \boldsymbol{u} = -\frac{1}{\rho}\nabla P - (\boldsymbol{u}\cdot\nabla)\boldsymbol{u} + \frac{1}{\rho}(\nabla\times\boldsymbol{b})\times\boldsymbol{b} + \nu\Delta\boldsymbol{u}, \quad (1)$$

$$\partial_t \boldsymbol{b} = (\boldsymbol{b}\cdot\nabla)\boldsymbol{u} - (\boldsymbol{u}\cdot\nabla)\boldsymbol{b} + \eta\Delta\boldsymbol{b}, \quad (2)$$

$$\nabla\cdot\boldsymbol{u} = 0 \quad \text{and} \quad \nabla\cdot\boldsymbol{b} = 0, \quad (3)$$

where $\boldsymbol{u}$ denotes the velocity field, $\boldsymbol{b}$ the magnetic induction expressed in Alfvén units, ν the kinematic viscosity, η the resistivity, P the pressure, and $\rho = 1$ the density. Equations (1)–(3) are numerically solved in a cubic domain of length $L = 2\pi$ with periodic boundary conditions using a fully dealiased pseudospectral MHD code, which we developed extending the hydrodynamic code of [14]. All simulations satisfy $k_{\max}\eta_{\mathrm{mag,kin}} \geqslant 1.26$, where $\eta_{\mathrm{mag,kin}}$ are the Kolmogorov scales associated with the magnetic and velocity fields, respectively. We do not impose a background magnetic field, and both the initial magnetic and velocity fields are random Gaussian with zero mean, with initial magnetic and kinetic energy spectra $E_{\mathrm{mag,kin}}(k) \sim k^4 \exp[-k^2/(2k_0)^2]$, unless otherwise specified. The peak wave number k_0 is varied for different simulations depending on the desired scale separation and resolution requirements. The initial relative magnetic helicity is $\rho_{\mathrm{mag}}(k) = kH_{\mathrm{mag}}(k)/2E_{\mathrm{mag}}(k) = 1$, the initial cross helicity is negligible, and the initial velocity field is nonhelical, unless otherwise specified. The ratio between magnetic and kinetic energies $\Gamma(t) = E_{\mathrm{kin}}(t)/E_{\mathrm{mag}}(t)$ equals unity at $t = 0$, where $E_{\mathrm{mag,kin}}(t) = \int dk\, E_{\mathrm{mag,kin}}(k,t)$. All spectral quantities have been shell and ensemble averaged. Results have been obtained for a range of Reynolds numbers; the figures show data from the highest resolved simulations only. A summary of simulation details is shown in Table I; further details including benchmarking against results in the literature [15,16] can be found in [17].

The numerous single realization studies of RST make it evident that it should also appear as a property in ensemble-averaged data, but this is the first analysis to adopt this procedure. In isotropic hydrodynamic turbulence it is pointed out in [18] that the direct cascade of kinetic energy is an ensemble-averaged concept and in [19] that a single realization

*ab@ph.ed.ac.uk

†m.linkmann@ed.ac.uk

[1]The alternative terminology "inverse cascade" might be inaccurate as it implies spectral locality [12].

TABLE I. Specifications of simulations. H and NH refer to initially helical and nonhelical magnetic fields, respectively. The additional letter "d" refers to the decoupled system, η denotes the magnetic resistivity, k_0 the peak wave number of the initial energy spectrum, and # the ensemble size.

Run id	N^3	$R_\lambda(0)$	$10^3\eta$	k_0	#	$t_{\max}$
H1-8,10	128^3-528^3	28.69-258.19	9-1	5-15	10	50
H9	1024^3	74.84	0.75	23	10	6
H11	1032^3	645.47	0.4	5	5	22
NH1-6	128^3-512^3	28.69-172.13	9-1.5	5	10	10-50
Hd1-4	256^3-528^3	43.03-57.38	6-4.5	5	10	5
Hd5	1032^3	28.06	2	23	10	2
NHd1-3	256^3-512^3	43.03-57.38	6-4.5	5	10	5

could show energy transfer towards small wave numbers, and it is the mean kinetic energy transfer that proceeds from low to high wave numbers. At low k, the regime important for RST, shell averaging is not an optimal averaging method, since there is only a small number of points to average over. Furthermore, the modes in a given k shell do not evolve independently from each other, as they become increasingly correlated by nonlinear mode coupling, whereas different realizations in an ensemble are statistically independent. It has also been noted that the actual measuring process in experimental studies of decaying turbulence results in an ensemble average [8].

Our ensemble-averaged results for $E_{\rm mag}(k)$ and $H_{\rm mag}(k)$ at different times are shown in Fig. 1 for run H9 in Table I, where the helicity spectra have been shifted for easier comparison. Error bars have been omitted to facilitate visual comparison between spectra at different times, but it should be noted that the measured spectra do not lie within the error of one another. The inset of Fig. 1 shows the flux of magnetic helicity $-\Pi_H(k) = \int_0^k dk'\, T_H(k')$, where $T_H(k')$ denotes the transfer spectrum of the magnetic helicity [9], at one and five initial large eddy turnover times t_0 in the very low k region. It is positive [as is $H_{\rm mag}(k)$ at all times], which again indicates RST,

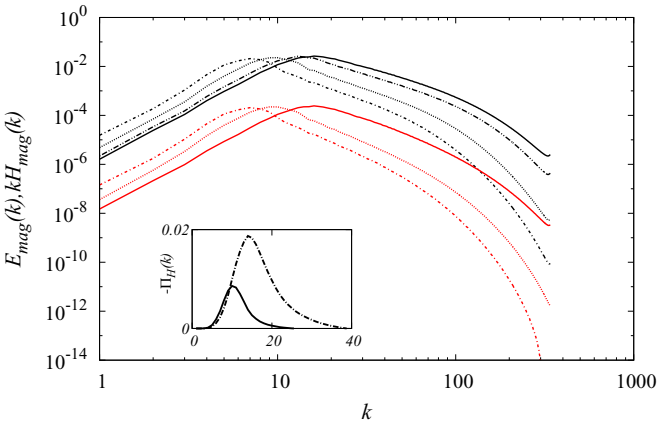

FIG. 1. (Color online) Magnetic energy and helicity spectra of run H9 showing reverse spectral transfer. The black (upper) lines refer to $E_{\rm mag}(k)$, and red (lower) lines to $kH_{\rm mag}(k)$. Solid lines indicate one initial turnover time t_0; dotted and dash-dotted lines refer to $2t_0$, $5t_0$, and $10t_0$. The inset shows the flux of magnetic helicity at t_0 and $5t_0$.

but not constant. This indicates the absence of an inertial range, hence the observed RST here cannot be named a cascade. This is in accord with standard results in this wave-number range; an inertial range is not expected at the very low k [12]. For visual purposes, we show a low R_λ result, which allows for higher scale separation at the low wave numbers. Higher R_λ results showing an inertial range for the magnetic helicity in the higher k direct cascade region can be found in [17].

RST can also be studied through $E_{\rm mag}(t)$ and $E_{\rm kin}(t)$. Since RST sends magnetic energy from small length scales back to large length scales, where dissipation is smaller, $E_{\rm mag}(t)$ should decay slower than $E_{\rm kin}(t)$. There is agreement in the MHD literature that $E_{\rm kin} \sim t^{-1}$ [5,10,20–22]. For $E_{\rm mag} \sim t^{-n_E}$ in helical MHD turbulence decay there are conflicting results on the decay exponent n_E, with two asymptotic decay laws proposed. One model assumes equipartition of $E_{\rm kin}(t)$ and $E_{\rm mag}(t)$ during turbulence decay [10], leading to the asymptotic decay law $E_{\rm mag}(t) \sim t^{-2/3}$. The second model proposes $E_{\rm mag} \sim E_{\rm tot}(t) \sim t^{-1/2}$ and has been derived in [10,22] as an asymptotic decay law for the *total* energy with respect to late times in the decay when the decreasing ratio $\Gamma = E_{\rm kin}/E_{\rm mag}$ is small, thus not assuming equipartition. Both decay laws have been observed to a good approximation for runs at specific Reynolds numbers [5,10,22,23]. One case [24] studied a range of low Reynolds numbers and attempted an extrapolation which supported the second model.

Ensemble averaging permits a straightforward means to compute the statistical error on the measured quantity, here n_E, whereas with a single realization the only error one can obtain is the error on the fit. Furthermore, for high resolution simulations one usually assumes that the ensemble average can be replaced with the volume average of one realization. Since RST generates long-range correlations, different regions in space will eventually become statistically correlated and the volume average will not reflect this. We observed that the energy spectra and the derived decay curves showed little deviations between realizations for $t < 7t_0$, while around $t \geq 7t_0$ the deviations became significant. As an example, for run H2 n_E varied from 0.81 to 0.96 between realizations if measured for $t > 7t_0$. Further details can be found in [17].

We measured n_E for an $R_\lambda(0)$ range of 28.69–645.47 using ensembles of typically ten runs on up to 1032^3 grid points (see Table I), with our results in Fig. 2. The largest simulation H11 was run up to $t = 27t_0$, while the lower resolved runs reached $t = 64t_0$. As shown in the figure, we find n_E has a $1/R_\lambda$ dependence. Extrapolating from this data to the infinite Reynolds number limit results in an asymptotic decay law $E_{\rm mag}(t) \sim t^{-n_{E,\infty}}$ with $n_{E,\infty} = 0.47 \pm 0.03$. These results show that decay of magnetic energy in a helical system is slower than kinetic energy, thus supporting the presence of RST. Moreover, our asymptote is consistent with the second model mentioned above [10,22] and is unambiguously not consistent with the first model. As can be seen in the inset of Fig. 2, the ratio $\Gamma(t) = E_{\rm kin}(t)/E_{\rm mag}(t)$ decreases over time. Our results also go further than [10,22] as they yield finite Reynolds number results and a $1/R_\lambda$ dependence of n_E. A Reynolds number dependence of n_E consistent with $n_{E,\infty} = 1/2$ had been found before [24], albeit at much lower resolution using Reynolds numbers defined with respect to a length scale associated with the helicity. We also found that the

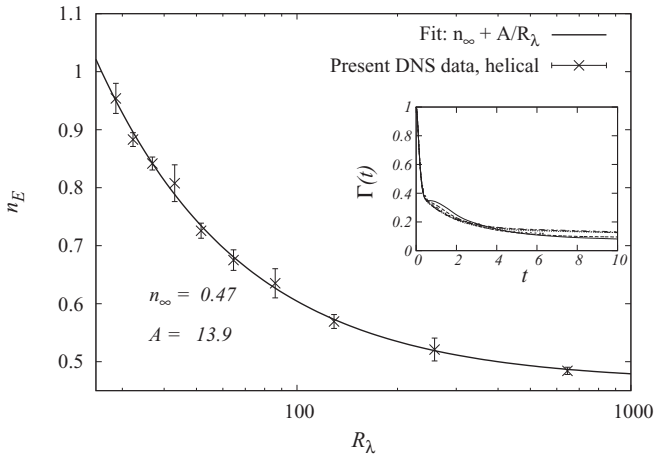

FIG. 2. Reynolds number dependence of decay exponents of $E_{\rm mag}(t)$ for maximally helical initial magnetic fields. The inset shows the decay of $\Gamma(t)$ for runs H3-H11.

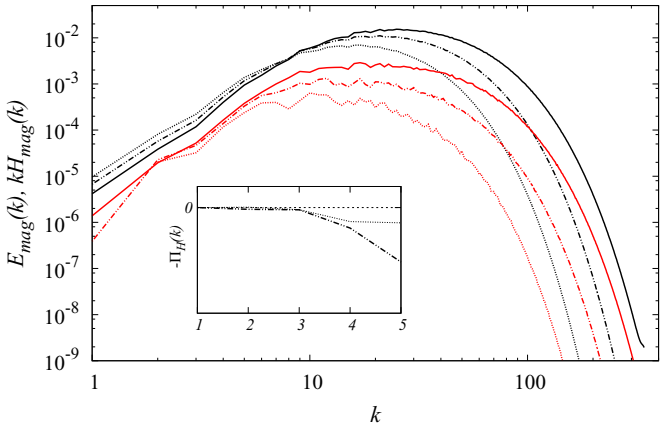

FIG. 3. (Color online) Magnetic energy spectra showing reverse spectral transfer for the decoupled system (run Hd5). Note the absence of RST for the magnetic helicity. The black (upper) lines refer to $E_{\rm mag}(k,t)$, the red (lower) lines to $kH_{\rm mag}(k,t)$, and the solid lines are earlier in time than the dotted lines. The inset shows the flux of magnetic helicity.

evolution of the integral scale approaches $L_{\rm mag}(t) \sim t^{1/2}$ (not shown). This is consistent with the approximate conservation of magnetic helicity at large magnetic Reynolds number, since $H_{\rm mag}(t) \sim E_{\rm mag}(t) L_{\rm mag}(t)$ [9].

For the nonhelical case we have done a small analysis in response to [25] for ensembles of 10 runs on up to 512^3 grid points, resulting in exponents consistent with $E_{\rm mag}(t) \sim t^{-1}$, in agreement with [4,5,20] and the theoretical analysis by Campanelli [21]. Since the decay exponents of $E_{\rm kin}(t)$ and $E_{\rm mag}(t)$ coincide for a nonhelical magnetic system, if one field shows RST so should the other, provided RST is large enough to influence the time evolution of the system. Brandenburg *et al.* [25] recently reported RST of magnetic and kinetic energies from a single realization run of an initially nonhelical magnetic system on 2304^3 grid points. Our ensemble of runs shows similar behavior for the magnetic energy.

To further investigate RSTs we made an *ad hoc* modification of the momentum equation (1) by omitting the Lorentz force $(\boldsymbol{\nabla} \times \boldsymbol{b}) \times \boldsymbol{b}$, which decouples the velocity field from the magnetic field. This approach clearly does not lead to a faithful representation of MHD, since the decoupled fluid-magnetic field system ceases to be energetically closed. Its purpose is to serve as a diagnostic tool to unravel the complicated nonlinear set of equations to allow an understanding of the mathematical properties of the induction equation (2) as a linear partial differential equation. In particular, one can test if RST is among those mathematical properties.

The logic behind this modification can be viewed in another way. One can solve the full MHD equations and store the $\boldsymbol{u}(\boldsymbol{x},t)$ solution. One can imagine now doing this slightly differently by solving just the induction equation with the same initial conditions using the above stored $\boldsymbol{u}(\boldsymbol{x},t)$ function. In both cases one obtains exactly the same solution for $\boldsymbol{b}(\boldsymbol{x},t)$. However, in the second case it was through the solution of a linear partial differential equation with variable coefficients, here given by $\boldsymbol{u}(\boldsymbol{x},t)$. The step made here is to provide an alternative viewpoint, that is, the entire problem of RST can be analyzed through solving a linear partial differential equation with variable coefficients. This is still a hard problem, but now linear and thus tractable. One way forward is to dismiss the MHD equations and study the induction equation in isolation with different external $\boldsymbol{u}$ fields, as a means to probe this equation for features that produce RST. That is what we did here with perhaps the most obvious initial example of an independently evolving turbulent $\boldsymbol{u}$ field, and as will be shown below, have found even in that case, the induction equation leads to RST.

We have conducted simulations for this decoupled system on up to 1032^3 grid points with our results shown in Fig. 3 for an ensemble of 10 runs. As seen in this figure, there is a RST of magnetic energy, which is interesting since it emerges from a linear equation. To diminish the possibility of a finite-size effect, we set the peak of the initial spectra relatively high, e.g., in Fig. 3, $k_0 = 23$. Moreover, we have done several tests [17] to verify this linear RST, such as reproducing the same effect in slightly compressible MHD using the PENCIL CODE [26].

Interestingly, we do not find RST of magnetic helicity in these simulations. The reverse transfer of $E_{\rm mag}(k,t)$ is usually thought to be driven by the reverse transfer of $H_{\rm mag}(k,t)$ by virtue of the realizability condition $|H_{\rm mag}(k,t)| \leq 2E_{\rm mag}(k,t)/k$ [9]. Our results show that RST of magnetic energy is possible without RST of magnetic helicity, despite the magnetic field being initially maximally helical. Although some realizations showed RST of $H_{\rm mag}(k,t)$ at $k = 1$ and there appears to be a hint of RST at $k = 2$, the ensemble average strongly supports the absence of RST of $H_{\rm mag}(k,t)$. The data point at $k = 2$ lies within the error of the ensemble-averaged data at earlier time. The flux of magnetic helicity is shown in the inset of Fig. 3 to be negative at low k, thus indicating the absence of RST, as opposed to the coupled case shown in Fig. 1, where it is positive at low k.

As the velocity field is not influenced by the magnetic field in this decoupled system and is initially nonhelical for the results in Fig. 3, effects of kinetic helicity could not influence the evolution of the magnetic field. However having decoupled these two equations, it permits us to cleanly test the influence

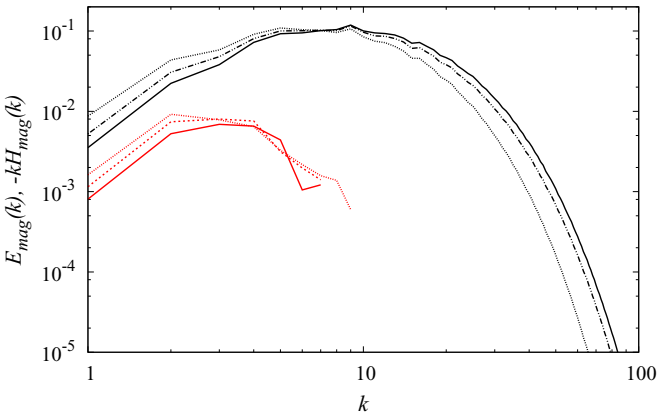

FIG. 4. (Color online) Magnetic energy and helicity spectra for the decoupled case Hd4 showing RST for an initially helical velocity field. The black (upper) lines refer to $E_{\rm mag}(k,t)$, the red (lower) lines to $-kH_{\rm mag}(k,t)$, and the solid lines are earlier in time than the dotted lines. Since $H_{\rm mag}(k,t)$ is positive at larger k, it does not show on logarithmic scales.

that kinetic helicity can have on the magnetic system. In Fig. 4 our initial $\boldsymbol{u}$ and $\boldsymbol{b}$ fields were set to be maximally helical in the same direction and now we observe RST of both magnetic energy and helicity. In particular, this simulation was started with $H_{\rm mag}(k) > 0$ for all $k > 0$, and we found the magnetic helicity to increase at large wave numbers while it decreased at low wave numbers, eventually changing sign. The now negative magnetic helicity is subsequently transferred to lower k. This suggests that RST of magnetic helicity relies on the presence of kinetic helicity, which hints at a connection between large-scale dynamo action and RST of $H_{\rm mag}(k,t)$.

We also examined in our decoupled equations the case of an initially nonhelical magnetic field. Two cases were investigated here: one with $E_{\rm mag}(k,0) = E_{\rm kin}(k,0) \sim k^4$ at low k and one with $E_{\rm kin}(k,0) \sim k^2$ while $E_{\rm mag}(k,0) \sim k^4$ at low k as in [25]. We found RST in both cases, more pronounced in the second than in the first case. These results further support the findings in [25,27] on nonhelical RST, now also for our linear RST.

A plausible explanation of these observations would be that RST of magnetic energy has two components: a dominant (nonlinear) one due to the reverse transfer of magnetic helicity and a residual (linear) one which is slightly augmented by the presence of magnetic helicity. Our numerical results show that coupling between helical modes has an impact on RST, especially if the coupling includes helical $\boldsymbol{u}$ modes. For initially helical $\boldsymbol{u}$ fields we also saw that coupling between positively helical $\boldsymbol{b}$ and $\boldsymbol{u}$ modes led to a positively helical magnetic field becoming negatively helical. Decomposing both fields into helical modes to study the mode couplings might lead to further insight.

In order to understand the physical nature of RST, an analytic study of the induction equation as a linear partial differential equation in this decoupled system might lead to further insight and can serve to get a step further towards the full nonlinear problem. The induction equation can be further studied using classical techniques such as Green's functions and integral transforms. One could further dissect it by retaining one of the transfer terms only. If the advective term $(\boldsymbol{u}\cdot\nabla)\boldsymbol{b}$ is retained, we obtain an advection-diffusion equation, which has been extensively studied in the literature. The nature of the linear RST would be different depending on which of the transfer terms produces it, and this could inspire models to be put forward that highlight physical processes responsible for the full nonlinear RST, which is analytically intractable. In the case of the kinetic source term $(\boldsymbol{b}\cdot\nabla)\boldsymbol{u}$, RST would be a transfer of *kinetic* to magnetic energy, while in the case of the advective term the transfer would be of magnetic energy only.

In summary, this Rapid Communication presented the first ensemble-averaged measurements of reverse spectral transfer of magnetic energy and helicity, which show that these forms of transfer are statistical properties of the MHD equations. Our analysis showed that at early times single realization measurements are sufficient to replicate the properties of the ensemble average, while at later times in the decay the ensemble average becomes a must, as we observed larger deviations between realizations. Turbulence decay is influenced by reverse spectral transfer; in the helical case we observed a Reynolds number dependence of the decay exponent $n_E = n_\infty + A/R_\lambda$ with $n_\infty \simeq 1/2$ and $A = 13.9 \pm 0.8$. The reverse transfers of magnetic energy and magnetic helicity were further investigated in a simplified system, which decoupled the evolution of the velocity field from the magnetic field. The magnetic helicity shows no reverse transfer in this system, and a new aspect of reverse transfer of magnetic energy was found, which is linear in nature and thus amenable to further mathematical analysis.

We thank David McComb for helpful advice on turbulence theory and numerical simulations. This work has made use of the resources provided by HECToR and ARCHER [28], made available through ECDF [29]. A.B. acknowledges funding from STFC, and M.L. is supported by EPSRC.

[1] A. Beresnyak, Phys. Rev. Lett. **108**, 035002 (2012); J. Cho, A. Lazarian, and E. T. Vishniac, in *Turbulence and Magnetic Fields in Astrophysics* (Springer, Berlin/Heidelberg, 2003), pp. 56–98; A. A. Schekochihin and S. C. Cowley, in *Magnetohydrodynamics-Historical Evolution and Trends* (Springer, Berlin, 2007), pp. 85–115.

[2] A. Brandenburg, K. Enqvist, and P. Olesen, Phys. Rev. D **54**, 1291 (1996).

[3] D. T. Son, Phys. Rev. D **59**, 063008 (1999).

[4] A. G. Tevzadze, L. Kisslinger, A. Brandenburg, and T. Kahniashvili, Astrophys J. **759**, 54 (2012).

[5] T. Kahniashvili, A. G. Tevzadze, A. Brandenburg, and A. Neronov, Phys. Rev. D **87**, 083007 (2013).

[6] S. M. Tobias, F. Cattaneo, and S. Boldyrev, in *Ten Chapters in Turbulence* (Cambridge University Press, Cambridge, 2013), pp. 351–404; J. Cho and E. T. Vishniac, Astrophys. J. **538**, 217 (2000); E. T. Vishniac and J. Cho, *ibid.* **550**, 752 (2001).

[7] R. S. Iroshnikov, Sov. Astron. **7**, 566 (1963); R. H. Kraichnan, Phys. Fluids **8**, 1365 (1965); P. Goldreich and S. Sridhar, Astrophys. J. **438**, 763 (1995).
[8] P. D. Mininni and A. Pouquet, Phys. Rev. E **87**, 033002 (2013).
[9] D. Biskamp, *Nonlinear Magnetohydrodynamics*, 1st ed. (Cambridge University Press, Cambridge, 1993).
[10] D. Biskamp and W.-C. Müller, Phys. Rev. Lett. **83**, 2195 (1999).
[11] W.-C. Müller and D. Biskamp, Phys. Rev. Lett. **84**, 475 (2000).
[12] W.-C. Müller, S. K. Malapaka, and A. Busse, Phys. Rev. E **85**, 015302 (2012).
[13] A. Pouquet, U. Frisch, and J. Léorat, J. Fluid Mech. **77**, 321 (1976).
[14] S. R. Yoffe, Ph.D. thesis, University of Edinburgh, 2012.
[15] P. D. Mininni, A. G. Pouquet, and D. C. Montgomery, Phys. Rev. Lett. **97**, 244503 (2006).
[16] J. A. Morales, M. Leroy, W. J. T. Bos, and K. Schneider, J. Comput. Phys. **274**, 64 (2014).
[17] See Supplemental Material at http://link.aps.org/supplemental/10.1103/PhysRevE.90.041003 for details and tests regarding the simulations.
[18] P. Sagaut and C. Cambon, *Homogeneous Turbulence Dynamics* (Cambridge University Press, Cambridge, 2008), p. 95.
[19] W. D. McComb, *Homogeneous, Isotropic Turbulence: Phenomenology, Renormalization and Statistical Closures* (Oxford University Press, Oxford, 2014), p. 82.
[20] M. Christensson, M. Hindmarsh, and A. Brandenburg, Phys. Rev. E **64**, 056405 (2001).
[21] L. Campanelli, Phys. Rev. D **70**, 083009 (2004).
[22] D. Biskamp and W.-C. Müller, Phys. Plasma **7**, 4889 (2000).
[23] S. K. Malapaka and W.-C. Müller, Astrophys. J. **778** 21 (2013).
[24] M. Christensson, M. Hindmarsh, and A. Brandenburg, Astron. Nachr. **326**, 393 (2005).
[25] A. Brandenburg, T. Kahniashvili, and A. G. Tevzadze, arXiv:1404.2238.
[26] See http://pencil-code.googlecode.com/.
[27] J. Zrake, arXiv:1407.5626v1.
[28] See http://www.hector.ac.uk/ and http://www.archer.ac.uk/.
[29] See http://www.ecdf.ed.ac.uk/.